

FLUCTUATIONS OF ELASTIC WAVES DUE TO RANDOM SCATTERING FROM INCLUSIONS*

V. A. KORNEEV and L. R. JOHNSON

*Center for Computational Seismology, Lawrence Berkeley National Laboratory,
University of California, Berkeley, California 94720, USA
E-mail: vakorneev@lbl.gov; lrj@ccs.lbl.gov*

Received 25 June 1999

Revised 28 March 2000

Exact solutions for elastic compressional and shear waves scattered from a homogeneous sphere are used to obtain formulas for fluctuations of velocity and attenuation of plane waves propagating through a layer of randomly distributed inclusions over a broad range of frequencies. The size and contrast of the inclusions are arbitrary, but interactions between scatterers are not considered and the concentration of scatterers is assumed to be small. The analytical solutions are also compared with numerical simulations and it is demonstrated that they satisfactorily explain the effects of scattering on both the mean and variance of the phase and the mean and variance of the attenuation. The need for spatial averaging of observational data and methods of interpreting such averaged data in terms of the material properties of the scattering medium are discussed.

1. Introduction

The problem of elastic wave propagation through heterogeneous media is encountered in numerous disciplines. It has been particularly important in the discipline of seismology because the earth is heterogeneous on a broad range of scales, and so a variety of different approaches to this problem have been developed. For a medium heterogeneous in only one dimension the problem is essentially solved because exact solutions exist, although even in this situation the process of estimating and describing the heterogeneity in realistic applications commonly introduces approximations. For media heterogeneous in two or three dimensions the problem is much more profound, as it is necessary to combine approximate solutions of the wave equations with approximate descriptions of the media, and understanding when a particular set of approximations is valid is not a simple matter.

Because of the complexity of heterogeneity within the earth, it is typically modeled as a random medium in which the effects of the heterogeneity upon elastic waves is treated in a statistical sense. Chernov⁴ was one of the first to adopt this description of the medium and then assumed scalar wave propagation in obtaining results that have been used in a variety of applications. See for example Aki,^{1–3} Wu,³⁰ Sato,^{25,26} and Flatté and Wu.⁶ Another common

*Presented at ICTCA'99, the 4th International Conference on Theoretical and Computational Acoustics, May 1999, Trieste, Italy.

approach is to use the Born approximation in which it is assumed that the perturbations in the elastic wave parameters are linearly related to the perturbations in the medium.

For examples of this approach in geophysics, see Knopoff and Hudson,^{15,16} Hudson,^{10,11} Sato,^{27,28} Wu and Aki,^{33,34} Wu,^{30,31} and Li and Hudson.^{22,23} Note also that there is a very large literature concerned with the scattering of waves in other fields (see for example Sheng,²⁹ Ishimaru,¹³ Lagendijk and Tiggelen.²¹) While these various approaches to the problem of wave propagation in heterogeneous media have been successful in certain applications, they are accompanied by important limitations which can raise questions about the validity and generality of the results. Examples of such limitations are the lack of conversions between modes of propagation, the failure to conserve energy, or the inability to handle strong contrasts in material properties. It is the purpose of this paper to present a method of handling wave propagation in three-dimensional heterogeneous media which avoids some of these limitations.

Fluctuations in wave fields due to randomness of the scattering media play an important role in acoustics, and their treatment was discussed in Chernov.⁴ Similarly, in elastic scattering problems the fluctuations of waves and their characteristics, such as an attenuation coefficient can be very strong causing “nonphysical” negative values, and therefore making reliable estimates of attenuation nearly impossible. For solid media the repeated experiments do not lead to a reduction in a fluctuation levels because the realization of the random medium is not changing in time. A reduction of elastic wave fluctuations is possible by spatial averaging of data. As it follows from the results of this paper the fluctuations themselves can be used to obtain information about media properties.

The basic approach followed in this paper is to treat the wave propagation process as a series of forward scattering problems. The medium is described as a random distribution of scatterers, where the size, material properties, and density of scatterers can vary. For the case where the scatterers are spherical and homogeneous, exact solutions for the single scattering process are used, but multiple scattering effects are only partly included due to use of an exact solution for a single scatterer and incident wave attenuation correction during its propagation. Therefore the results are applicable to the media with low concentrations of scatterers. The use of these exact scattering solutions allows a complete treatment of mode conversions between P and S waves and arbitrary strong contrasts in material properties. They also provide the starting point for deriving low-frequency and high-frequency asymptotic solutions that can be compared with other approximate solutions.

2. Scattering by a Single Inclusion

It is necessary to first review some of the results from single scattering theory. Consider a homogeneous material with elastic parameters and density given by $\lambda_2 \equiv \lambda$, $\mu_2 \equiv \mu$, $\rho_2 = \rho$. Velocities and wavenumbers for P and S waves, plus a velocity ratio, are defined by

$$v_p = \sqrt{\frac{\lambda + 2\mu}{\rho}}, \quad v_s = \sqrt{\frac{\mu}{\rho}}, \quad k_p = \frac{\omega}{v_p}, \quad k_s = \frac{\omega}{v_s}, \quad \gamma = \frac{v_s}{v_p}$$

where ω is angular frequency. At the origin of the coordinate system is a homogeneous inclusion having material properties λ_1, μ_1, ρ_1 , which are in general different from those of the surrounding material.

Consider a simple harmonic plane wave propagating in the direction of the positive z axis of a rectangular coordinate system (x, y, z) .

$$\tilde{\mathbf{u}}_{m0} = \mathbf{u}_{mo} e^{i\omega t}, \quad \mathbf{u}_{mo} = \hat{\mathbf{u}}_m u_{mo}, \quad u_{mo} = e^{-ik_m z} \quad (2.1)$$

Here the index $m = p, s$ denotes either an incident P wave ($m = p, v_m = v_p, \hat{\mathbf{u}}_m = \hat{\mathbf{z}}$) or an incident S wave ($m = s, v_m = v_s, \hat{\mathbf{u}}_m = \hat{\mathbf{x}}$).

The presence of the inclusion causes a disturbance of the incident wave which in spherical coordinate system is described by the scattered field $\mathbf{u}_{sc}^m(r, \theta, \phi)$. Thus the total field outside of the scatterer has the form

$$\mathbf{u}_m = \mathbf{u}_{mo} + \mathbf{u}_{sc}^m(r, \theta, \phi) = \mathbf{u}_{mp}(r, \theta, \phi) + \mathbf{u}_{ms}(r, \theta, \phi) \quad (2.2)$$

of scattered P and scattered S waves. The change in the incident wave amplitude due to the interaction with a single inclusion in the far field can be expressed as

$$\Delta u_m^{(1)} = (\mathbf{u}_m - \mathbf{u}_{mo}) \cdot \hat{\mathbf{u}}_m = u_{mo} [\mathbf{A}_{mm}(\theta, \phi)]_{c_m} \frac{e^{-ik_m(r-z)}}{r} \quad (2.3)$$

Note that in the far field the scattering function $\mathbf{A}_{mp}(\theta, \phi)$ is polarized along $\hat{\mathbf{r}}$ and orthogonal to $\mathbf{A}_{ms}(\theta, \phi)$ so that $(\mathbf{A}_{mp} \cdot \mathbf{A}_{ms}) = 0$. Index c_m denotes the principal far field component associated with the wave index m . For the geometry described above, $c_m = z$ for an incident P wave and $c_m = x$ for an incident S wave.

We also need a result relating the total energy in the scattered field to the forward scattered amplitude having the polarization of the incident wave, known as a forward scattering theorem or an optical theorem.⁹ Let F_{mo} be the energy flux per unit area averaged over one period and let Ω_1 be a closed spherical surface of unit radius surrounding the inclusion. Then it is easy to show that the scattering cross-sections related to the energy of the incident P and S waves are given by

$$\sigma_p \equiv \frac{F_{sc}^p}{F_{po}} = \int_{\Omega_1} (|\mathbf{A}_{pp}(\theta, \phi)|^2 + \gamma |\mathbf{A}_{ps}(\theta, \phi)|^2) d\Omega_1 = -\frac{4\pi}{k_p} \text{Im} \{[\mathbf{A}_{pp}(0, 0)]_z\} \quad (2.4)$$

$$\sigma_s \equiv \frac{F_{sc}^s}{F_{so}} = \frac{1}{\gamma} \int_{\Omega_1} (|\mathbf{A}_{sp}(\theta, \phi)|^2 + \gamma |\mathbf{A}_{ss}(\theta, \phi)|^2) d\Omega_1 = -\frac{4\pi}{k_s} \text{Im} \{[\mathbf{A}_{ss}(0, 0)]_x\} \quad (2.5)$$

3. Scattering by a Layer of Inclusions

Consider a thin slab extending to infinity perpendicular to the z axis between z and $z + \Delta z$. Inclusions having the same size, shape, and elastic properties are uniformly distributed within this slab with a density of $N(z)$, the number of inclusions per unit volume (Fig. 1).

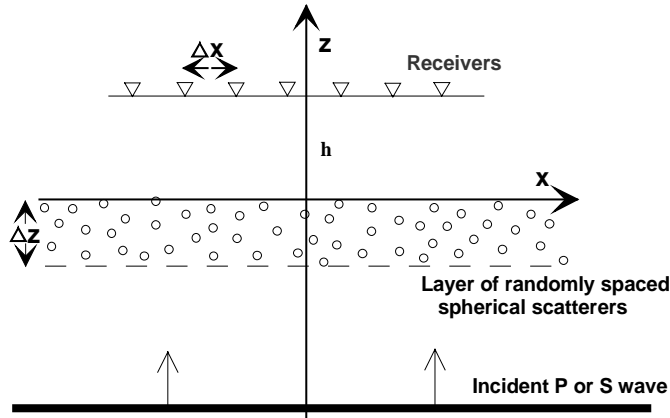


Fig. 1. The basic geometry for the scattering problems considered in this paper. A plane P or S wave propagating in the z direction encounters a thin slab of thickness Δz containing randomly distributed spherical scatterers having material properties different from the background medium. A distance h on the other side of the slab there is a line of receivers spaced a distance Δx apart in the x direction.

The average effect upon a plane wave propagating through this slab is obtained by summing up the effects of all the individual inclusions (Eq. (2.3))

$$\begin{aligned}\Delta \bar{u}_m(z + \Delta z) &= \Delta z \int_{-\infty}^{\infty} \int_{-\infty}^{\infty} N(z) \Delta u_m^{(1)}(x, y, z) dx dy \\ &= \Delta z N(z) \bar{u}_m(z) \int_{-\infty}^{\infty} \int_{-\infty}^{\infty} [\mathbf{A}_{mm}(\theta, \phi)]_{c_m} \frac{e^{-ik_m(r-z)}}{r} dx dy\end{aligned}\quad (3.1)$$

It is assumed in writing the above expression that the size and density of the inclusions is small enough so that scattering interactions between the inclusions can be neglected. Next we assume that the transmitted coherent plane wave is influenced only by the inclusions in a small cone about $\theta = 0$ which coincides with a few central Fresnel zones.¹² Then, approximating $\mathbf{A}_{mm}(\theta, \phi)$ by $\mathbf{A}_{mm}(0, 0)$ and using the parabolic approximation for the phase function $-k_m r$, we obtain

$$\Delta \bar{u}_m(z + \Delta z) = -i \Delta z \frac{2\pi}{k_m} N(z) A_m(z) \bar{u}_m(z) \quad (3.2)$$

where

$$A_m(z) \equiv [\mathbf{A}_{mm}(0, 0)]_{c_m}$$

is defined as the forward scattering coefficient at any value of z . In the limit as Δz becomes small this becomes the differential equation

$$\frac{d}{dz} \bar{u}_m(z) = -i \frac{2\pi}{k_m} N(z) A_m(z) \bar{u}_m(z) \quad (3.3)$$

This equation can be integrated for a layer having total thickness Z to obtain the net effect upon a plane wave passing through a layer ($0 \leq z \leq Z$) having inclusions distributed with

a density $N(z)$

$$\bar{u}_m(Z) = u_{mo} e^{-i \frac{2\pi}{k_m} \int_0^Z N(z) A_m(z) dz} \quad (3.4)$$

The result in Eq. (3.3) represents the average plane wave after it has propagated through a layer of thickness Z . It is sometimes referred to as the coherent part of the total field. A similar result was obtained by Groenenboom and Snieder⁸ for the two-dimensional scalar problem using the method of stationary phase.

The transmitted wave in Eq. (3.3) can also be expressed in the form (see Appendix B)

$$\bar{u}_m(Z) = u_{mo} e^{i \bar{\phi}_m(Z)} e^{-\bar{q}_m(Z)} \quad (3.5)$$

where the nondimensional phase shift $\bar{\phi}_m$ and attenuation \bar{q}_m are effective parameters which have the simple relationships

$$\bar{\phi}_m(Z) = \omega \Delta t_m(Z), \quad \bar{q}_m(Z) = \frac{\alpha_m(Z)}{2} Z \quad (3.6)$$

with an effective travel time deviation Δt_m and an effective scattering attenuation coefficient α_m . Then, comparing Eqs. (3.3) and (3.4), it is clear that

$$\bar{\phi}_m(Z) = -\frac{2\pi}{k_m} \int_0^Z N(z) \text{Re}\{A_m(z)\} dz \quad (3.7)$$

and

$$\bar{q}_m(Z) = -\frac{2\pi}{k_m} \int_0^Z N(z) \text{Im}\{A_m(z)\} dz \quad (3.8)$$

Using the optical theorem (2.4) for Eq. (3.7) we also have

$$\bar{q}_m(Z) = \frac{1}{2} \int_0^Z N(z) \sigma_m(z) dz \quad (3.9)$$

It is clear from Eqs. (3.8) and (3.5) that a local attenuation coefficient $\alpha_m(z)$ can be defined by

$$\alpha_m(z) = N(z) \sigma_m(z) \quad (3.10)$$

Equations (3.8) and (3.6) allow simple estimations of the time shift of the transmitted wave and correspondent effective velocity of random scattering medium.

The results contained in Eqs. (2.5) to (3.9) are generally true for any size of inclusion if the assumption of single scattering is justified. For the cases of one-dimensional scattering it was shown by O'Doherty and Anstey⁵ (1971) that incorporation of additional "peg-leg" paths to a single scattering solution gives very good approximation for a multiple scattering solution. In our case we include all scattering phenomena associated with the interaction of the incident wave with inclusions which contribute constructively to the coherent part of the total field. On the other hand, "peg-legs" corresponding to back scattered wave interaction between different scatterers are not coherent due to the randomness of scatterer

locations. Therefore for small concentrations they do not play a significant role in the total field characteristics. Another important condition is determined by the value of a “mean free path” $l_m = \alpha_m^{-1}$. For layer thicknesses Z exceeding l_m the result of single scattering approaches may not be valid due to destruction of the coherent part of the propagating field. In the following we assume that this condition is always satisfied. Note, that only scattering attenuation is included here, and intrinsic attenuation due to absorption of energy must be included separately.

4. Attenuation and Phase Fluctuations

In the previous section, formulas for the average attenuation and phase shift caused by propagation through a layer containing randomly distributed inclusions were derived. Because of the randomness involved in this problem, it is to be expected that there would be fluctuations about these average values if a series of experiments were performed for different realizations of the inclusion distribution. In order to estimate these fluctuations it is necessary to consider the squared scattering effect $\Delta|u_m|^2$ given by

$$\begin{aligned}\Delta|u_m|^2 &= |u_{mo} + \Delta u_m^{(1)}|^2 - |u_{mo}|^2 = 2\operatorname{Re}\{u_{mo}^* \Delta u_m^{(1)}\} + |\Delta u_m^{(1)}|^2 \\ &= 2|u_{mo}|^2 \operatorname{Re} \left\{ [\mathbf{A}_{mm}(\theta, \phi)]_{cm} \frac{e^{-ik_m(r-z)}}{r} \right\} + |\Delta u_m^{(1)}|^2\end{aligned}\quad (4.1)$$

The next step is to calculate the spatial average of this expression as the wave propagates through a thin slab of thickness Δz . The first term on the right presents no problem, as it is essentially the expression evaluated in Eq. (3.1). For the second term we keep the terms which are linear with respect of both small parameters Δz and concentration, and have

$$\begin{aligned}\overline{|\Delta u_m(z + \Delta z)|^2} &= \Delta z N(z) \int_{-\infty}^{\infty} \int_{-\infty}^{\infty} |\Delta u_m^{(1)}(x, y, z)|^2 dx dy \\ &= \Delta z N(z) \overline{|u_m(z)|^2} \int_{-\infty}^{\infty} \int_{-\infty}^{\infty} |[\mathbf{A}_{mm}(\theta, \phi)]_{cm}|^2 \frac{dx dy}{r^2}\end{aligned}$$

For the case where the scatterers are spheres of radius R , the forward scattering results are taken from Korneev and Johnson^{18,19} for contrast Mie scattering case and from Dubrovsky and Morozhnik⁶ for a low-contrast high frequency case. Evaluations of the resulting integrals are given in Appendix A, and we have

$$\overline{|\Delta u_m(z + \Delta z)|^2} = 2\pi \Delta z N(z) \overline{|u_m(z)|^2} |A_m(z)|^2 G_m \quad (4.2)$$

where G_m is a nondimensional function of frequency and elastic parameters. The complete expression for the averaged fluctuations is thus

$$\Delta \overline{|u_m(z + \Delta z)|^2} = \Delta z N(z) \overline{|u_m(z)|^2} \left[\frac{4\pi}{k_m} \operatorname{Im}\{A_m(z)\} + 2\pi |A_m(z)|^2 G_m \right] \quad (4.3)$$

which can also be written in terms of the scattering cross-section of Eq. (3.1) as

$$\Delta \overline{|u_m(z + \Delta z)|^2} = \Delta z N(z) \overline{|u_m(z)|^2} [-\sigma_m(z) + 2\pi |A_m(z)|^2 G_m] \quad (4.4)$$

In the low-frequency limit $k_m R \ll 1$ (Rayleigh scattering) Eq. (4.2) can be reduced to

$$\Delta \overline{|u_m(z + \Delta z)|^2} = \Delta z N(z) \overline{|u_m(z)|^2} [-\sigma_m(z) + 2\pi |A_m(z)|^2 G_m^{(0)}] \quad (4.5)$$

with constant $|G_m^{(0)}| < 1$. In the high-frequency limit $k_m R \gg 1$ it becomes

$$\Delta \overline{|u_m(z + \Delta z)|^2} = \Delta z N(z) \overline{|u_m(z)|^2} \left[-\sigma_m(z) + \frac{9\pi}{2k_m^2 R^2} |A_m(z)|^2 \right] \quad (4.6)$$

Using high frequency approximation from Dubrovsky and Morozhnik⁵ it is possible to obtain

$$\Delta \overline{|u_m(z + \Delta z)|^2} = \Delta z N(z) \overline{|u_m(z)|^2} \left[-\sigma_m(z) + \frac{4\pi}{k_m^2 R^2} |A_m(z)|^2 \right] \quad (4.7)$$

Equations (4.4) and (4.5) differ by the insignificant factor 1.125, which justifies the use of Eq. (4.2) for all frequencies, as long as we stay in the mean free path zone.

Consider the general result of Eq. (4.2) and take the limit as $\Delta z \rightarrow 0$ to obtain

$$\frac{d}{dz} \overline{|u_m(z)|^2} = N(z) [-\sigma_m(z) + 2\pi |A_m(z)|^2 G_m] \overline{|u_m(z)|^2} \quad (4.8)$$

Integrating this equation from $z = 0$ to $z = Z$ yields

$$\overline{|u_m(Z)|^2} = |u_{mo}|^2 e^{-\int_0^Z N(z) \sigma_m(z) dz} e^{2\pi \int_0^Z N(z) |A_m(z)|^2 G_m dz} \quad (4.9)$$

This result represents the fluctuations in the transmitted field after passing through a layer of arbitrary thickness Z .

The variance of the transmitted field is given by

$$\text{var}\{u_m(Z)\} = \overline{|u_m(Z)|^2} - |\bar{u}_m(Z)|^2 \quad (4.10)$$

and from Eqs. (3.6) and (3.1)

$$|\bar{u}_m(Z)|^2 = |u_{mo}|^2 e^{-\int_0^Z N(z) \sigma_m(z) dz} \quad (4.11)$$

Thus

$$\text{var}\{u_m(Z)\} = |u_{mo}|^2 e^{-\int_0^Z N(z) \sigma_m(z) dz} \left[e^{2\pi \int_0^Z N(z) |A_m(z)|^2 G_m dz} - 1 \right] \quad (4.12)$$

This expression clearly shows the two competing effects that control the fluctuations in the transmitted field. The term in brackets, which represents the conversion of energy from the coherent field into random fluctuations, starts from zero when $Z = 0$ and grows continuously as Z increases. This growth is tempered by the decaying term in front of the brackets, representing the continuous loss of energy from the coherent field caused by the scattering. As is shown below, the combination of these two effects leads to a maximum in the fluctuations at a particular value of Z .

Note that another method of characterizing the relative size of the fluctuations is in terms of a coefficient of variation defined as

$$\text{COV} = \left[\frac{\text{var}\{u_m(Z)\}}{|\bar{u}_m(Z)|^2} \right]^{1/2} = \left[e^{2\pi \int_0^Z N(z)|A_m(z)|^2 G_m dz} - 1 \right]^{1/2} \quad (4.13)$$

This result shows that the relative size of the fluctuations grows monotonically with the distance of propagation.

It is shown in Appendix B that the average squared value of the phase shift of Eq. (3.6) and the attenuation of Eq. (3.7) are equal to each other and have the value

$$\overline{|\phi_m(Z)|^2} = \overline{|q_m(Z)|^2} = \pi \int_0^Z N(z)|A_m(z)|^2 G_m dz \quad (4.14)$$

When the high frequency result of Eq. (4.4) is used in place of Eq. (4.2), the variance becomes

$$\text{var}\{u_m(Z)\} = |u_{mo}|^2 e^{-\int_0^Z N(z)\sigma_m(z)dz} \left[e^{\frac{4\pi}{k_m^2} \int_0^Z N(z) \frac{|A_m(z)|^2}{R^2} dz} - 1 \right] \quad (4.15)$$

Numerical calculations at high frequencies reveal that in general

$$\text{Im}\{[\mathbf{A}_{mm}(0,0)]_{c_m}\} \gg \text{Re}\{[\mathbf{A}_{mm}(0,0)]_{c_m}\}$$

and therefore from Eq. (2.4) it follows that

$$|A_m(z)|^2 \approx |\text{Im}\{[\mathbf{A}_{mm}(0,0)]_{c_m}\}|^2 = \left(\frac{k_m \sigma_m(z)}{4\pi} \right)^2$$

Substituting this into Eq. (4.13) results in

$$\text{var}\{u_m(Z)\} = |u_{mo}|^2 e^{-\int_0^Z N(z)\sigma_m(z)dz} \left[e^{\frac{1}{4\pi} \int_0^Z N(z) \frac{\sigma_m^2(z)}{R^2} dz} - 1 \right] \quad (4.16)$$

A further simplification is possible if we use an asymptotic expression for the scattering cross-section $\sigma_m \approx 2\pi R^2$ when $k_m R \rightarrow \infty$ to obtain

$$\text{var}\{u_m(Z)\} = |u_{mo}|^2 e^{-2\pi \int_0^Z N(z)R^2 dz} \left[e^{\pi \int_0^Z N(z)R^2 dz} - 1 \right] \quad (4.17)$$

When the inclusions are all uniform with respect to size, elastic parameters, and density, the result for high frequencies reduces to the simple form

$$\text{var}\{u_m(Z)\} = |u_{mo}|^2 e^{-2\pi N R^2 Z} [e^{\pi N R^2 Z} - 1] \quad (4.18)$$

This result says that for scatterers large compared to the wavelength of the incident wave, the fluctuations in the scattered field are independent of frequency and proportional to the density of scatterers N and the squared radius of the inclusions.

Consider again the general expression for the variance given in Eq. (4.13). It is straightforward to show in both of the limit cases $\omega \rightarrow 0$ and $\omega \rightarrow \infty$ that

$$2\pi |A_m(z)|^2 G_m < \sigma_m(z)$$

Although an analytical demonstration has not yet been found, numerical calculations indicate that this result holds for all frequencies. Assuming this to be true in general, it follows that $\text{var}\{u_m(Z)\} \rightarrow 0$ as $Z \rightarrow \infty$. From Eq. (4.13) it is obvious that $\text{var}\{u_m(Z)\} \rightarrow 0$ as $Z \rightarrow 0$. Thus the variance must have a maximum at some intermediate value $Z = \hat{Z}$. The condition for this maximum is

$$2\pi \int_0^{\hat{Z}} N(z)|A_m(z)|^2 G_m dz = \ln \left[\frac{\sigma_m(\hat{Z})}{\sigma_m(\hat{Z}) - 2\pi|A_m(\hat{Z})|^2 G_m} \right] \quad (4.19)$$

Introducing the concentration $c(z) = (4\pi/3)R^3 N(z)$ as the fraction of the volume occupied by inclusions and assuming that it and the inclusion properties are constant at low frequencies leads to

$$c \frac{\hat{Z}}{R} = \frac{8k_m^2 R^4}{27\pi|A_m|^2} \ln \left[\frac{\sigma_m}{\sigma_m - 2\pi|A_m|^2 G_m} \right] \quad (4.20)$$

5. Numerical Modeling of Scattering

The effect of scattering on propagating plane elastic waves was simulated by using the exact scattering solution for a single elastic sphere.^{17,19} The design of the experiment is shown in Fig. 1. A thin slab of a scattering medium having thickness Δz was simulated by distributing a large number of spherical inclusions having the same radius R and with random spacing so that the z coordinates of all the centers of the spheres were in the interval $(-\Delta z, 0)$. Plane elastic P and S wave pulses containing a broad (0.4–100 Hz) range of frequencies were propagated in the positive z direction. Offset a distance h from the scattering region, were a set of K receivers having a separation interval of Δx . The lateral size of the box, $20 \text{ km} \times 20 \text{ km}$, was taken large in comparison to h and Δx in order to achieve the effect of a layer having infinite extent. The concentration was taken to be $c = 10\%$, which required a rather large number of scatterers $N = 5300$. The other parameters used were $h = 4 \text{ km}$, $R = 0.1 \text{ km}$, $\Delta z = 0.5 \text{ km}$ and $\Delta x = 0.5 \text{ km}$. The material properties of the background medium were $v_{p2} = 5.3 \text{ km/s}$, $v_{s2} = 3.2 \text{ km/s}$, $\rho_2 = 2.65 \text{ gm/cm}^3$ and for the scatterers they were $v_{p1} = 3.0 \text{ km/s}$, $v_{s1} = 2.0 \text{ km/s}$, $\rho_1 = 2.6 \text{ gm/cm}^3$. For the chosen parameters the layer thickness never exceeded one half of the mean free path.

Equations (3.7) and (3.8) were used to estimate the attenuation parameter $\Delta \bar{q}_m(z + \Delta z)$ from the modulus and the phase shift parameter $\Delta \bar{\phi}_m(z + \Delta z)$ from the phase. The results for P incident wave are shown as dotted lines in Fig. 2. The calculations were performed on a single seismogram (upper panels in the figures) and for the average of all 20 seismograms (lower panels in the figures). Note that the phase is ambiguous by multiples of 2π and this ambiguity can sometimes be removed by searching for discontinuities. This unwrapping of the phase was attempted for the phase calculated from the averaged seismogram, but not for that of the single seismogram where the high degree of randomness in the data did not permit a stable result. Also shown in Figs. 2 are the analytical estimates for the attenuation and phase calculated from Eqs. (3.6) and (3.7) (heavy solid lines) and the analytical estimates for the fluctuations calculated from Eq. (4.2) (light solid lines shown as plus and minus one

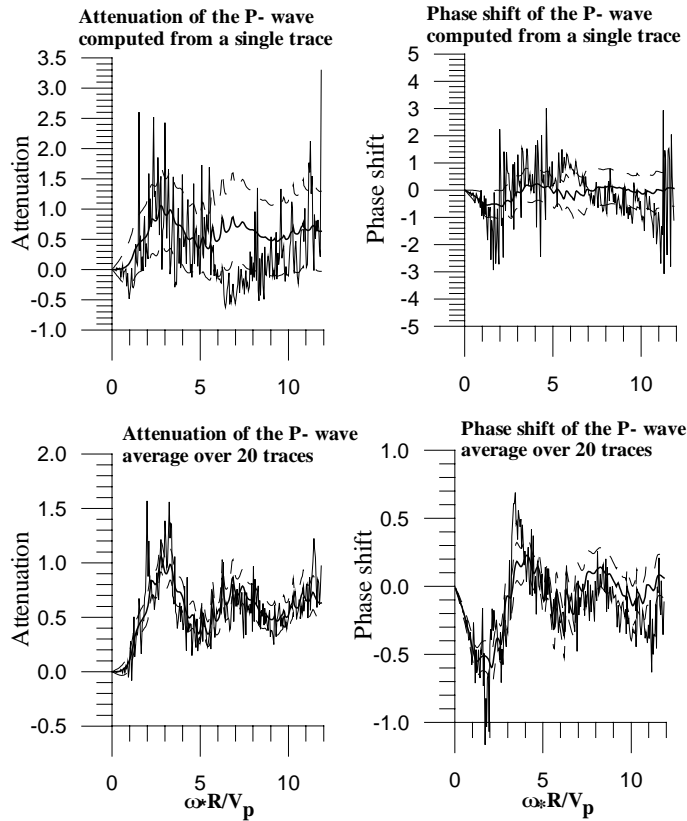


Fig. 2. Scattering characteristics for an incident P wave as calculated using synthetic data where the results for a single seismogram are shown in the upper panels (a) and (b) and the results for the average of all the seismograms are shown in the lower panels (c) and (d). The results are shown as light solid lines, while analytical estimates for the mean values are shown as heavy solid lines and analytical estimates for the mean plus and minus one standard deviation are shown as broken solid lines.

standard deviation). For the comparison with the average seismograms it was assumed that the fluctuations accumulated uncorrelated so that the variance of the average decreased as K^{-1} , where $K = 20$ was the number of seismograms that were averaged. The results for S incident wave look quite similar.

These results as well as a number of other results obtained for a variety of parameters including the presence of liquid filled inclusions and voids form the basis for several general observations. First, the analytical estimates are in reasonable agreement with the numerical results for both the mean and variance. For a single seismogram the statistical uncertainty is so large that only general trends can be identified, but in the case of the averaged seismograms a much more quantitative evaluation of the agreement can be performed. The agreement is slightly better for the attenuation than for the phase, which contains the additional complication of phase unwrapping. An associated observation is that, due to the statistical fluctuations, it may be impractical in many situations to reliably estimate attenuation and phase from a single seismogram, and the advantages of using spatially averaged data are significant.

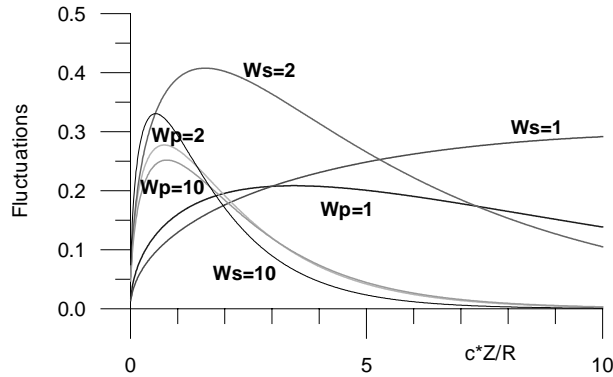


Fig. 3. Amplitude of the fluctuations as a function of the nondimensional distance of propagation cZ/R , where R is the radius of the scatterers, c their concentration, and Z the distance of propagation. The results are shown for various values of the nondimensional frequency $W_m = \omega R/v_m$. The material properties are the same as those used in Fig. 2.

A second general observation is that the results exhibit relatively simple behavior at low frequencies where the wave parameter is less than about 2. In this range the numerical and analytical results are in good agreement (even for a single seismogram) and the phase shows a linear dependence upon frequency. The third general observation concerns the behavior at high frequencies. Although there are both long and short wavelength oscillations in the results that are associated with the dimensions and properties of the scatterers, the trend in the attenuation is a constant nonzero value and the trend in the phase is a constant value of about zero.

In the discussion following Eq. (4.13) it was pointed out that, due to the competing effects of conversion of energy from the coherent field and the resultant decay of the coherent field, the amplitude of the fluctuations in the transmitted field will have a maximum at a particular propagation distance. Note that an expression for the maximum is given in Eq. (6.5), but this is not a particularly simple function of either frequency or wave type. This phenomenon is shown for various values of frequency in Fig. 3.

It is clear that the fluctuations rise from a value of zero at small distances and decay to zero again at large distances, which requires that there be a maximum at some intermediate distance. It appears that the distance to the maximum decreases as the frequency increases. It also appears in this figure that the distance to the maximum is greater for S waves than P waves at low frequencies.

6. Discussion and Conclusions

The analytical results of this paper provide a method of estimating the effects of scattering upon a plane wave propagating through a layer of randomly distributed spherical inclusions. Formulas have been obtained for both the average field and the statistical fluctuations about this average. The general results can be used for inclusions of arbitrary size and contrast and for all frequencies, as long as the thickness of the slab does not exceed a mean free path, but approximations for small inclusions or low contrast inclusions have also been included. These

analytical results have been validated by comparing them with effective media estimates at low frequencies and with numerical simulations over the entire frequency range. In both cases the agreement is satisfactory, which suggests that appropriate approximations were used in evaluating the various integrals encountered in the theoretical development.

The results displayed in Fig. 2 show that the relatively simple expressions of Eqs. (3.6) and (3.7) do an acceptable job over a broad frequency range of describing phase and attenuation effects upon a wave propagating through a region containing scatterers. The fluctuations calculated with Eq. (4.13) also serve as adequate bounds on the statistical uncertainty of the mean field.

Because of the random fluctuations, any attempt to reliably estimate the characteristics of the scattering on the basis of a single seismogram may be a difficult task. Only the phase shift at low frequencies shows a reasonable approximation to the mean field. Note that nonphysical negative values of attenuation are common in the results for a single seismogram. This means that in most cases some sort of spatial averaging of the observational data will be necessary before stable values of the mean phase and attenuation can be estimated. Assuming that an averaging process has been applied which has reduced the fluctuations to a acceptable fraction of the mean value, it is of interest to consider how data such as that shown in Fig. 2 can be interpreted in terms of material properties of the scattering medium. Measurements at high frequencies of velocity (or phase) are only dependent upon the background medium and thus can be used to estimate v_{p2} , v_{s2} , and ρ_2 . Measurements of velocity at low frequencies²⁰ can provide constraints on the properties of the inclusions v_{p1} , v_{s1} , ρ_1 and the concentration c . The first peak in the phase curve is a well-defined feature and constraints on the material properties can be obtained by fitting the analytical results to the data. For instance, in the low-contrast case it can be shown that the position of this first peak is given by

$$\omega_{\text{peak}} \approx 2.8 \frac{v_{m2}}{2R} \left(\frac{v_{m2}}{v_{m1}} - 1 \right)^{\frac{1}{2}} \quad (6.1)$$

Similar constraints are provided by measurements of attenuation. Using Eq. (3.8), and assuming a uniform distribution of the concentration and type of inclusions, we have

$$\bar{q}_m(Z) = \frac{3cZ}{8\pi R^3} \sigma_m \quad (6.2)$$

At low frequencies (Rayleigh regime) where the attenuation is rapidly increasing, the proportionality of $\sigma_m \sim \omega^4 R^6$ can be used to obtain

$$\bar{q}_m(Z) \sim cR^3 Z \omega^4 \quad (6.3)$$

Fitting this expression to the attenuation places constraints on c and R . At high frequencies ($k_m R \gg 1$) where the attenuation is approximately constant the limiting value of $\sigma_m = 2\pi R^2$ leads to

$$\bar{q}_m(Z) = \frac{3cZ}{4R} \quad (6.4)$$

This is second constraint on c and R provided by the attenuation data, which means that independent estimates of these two parameters are possible. Note that in the limit of high frequencies the attenuation data are independent of the velocities and densities.

Some information about the properties of the scattering medium can also be extracted from the level of the fluctuations. At high frequencies this level becomes independent of frequency. Noting that the mean value of the phase goes to zero in this range, one can start with Eq. (4.12) and use the same arguments that led to Eq. (4.16) to obtain

$$\text{var}\{\phi_m(Z)\} = \frac{\pi N R^2 Z}{2} = \frac{3cZ}{8R} \quad (6.5)$$

This provides another constraint on c and R .

In this paper the attenuation has been described with the nondimensional attenuation \bar{q}_m or the attenuation parameter α_m . Another common method of defining attenuation is in terms of the quality factor Q . The relationships between the various definitions are

$$Q_m^{-1} = \frac{2v_m}{\omega Z} q_m = \frac{v_m}{\omega} \alpha_m = \frac{v_m}{\omega} N \sigma_m = \frac{3cv_m}{4\pi\omega R^3} \sigma_m$$

Using the same limits discussed above, at low frequencies we have

$$Q_m^{-1} \sim cR^3\omega^3$$

and at high frequencies

$$Q_m^{-1} = \frac{3cv_m}{2\omega R}$$

The results of this paper have been demonstrated with calculations and examples that assumed inclusions having the same type and size, but the results are much more general than this. For instance, in the basic results of Eqs. (3.6), (3.7), and (4.2) the critical elements are integrals involving expressions of the form $N(z)F\{A_m(z)\}$, where $N(z)$ is the density of scatterers having the forward scattering coefficients $A_m(z)$ and F is some function of A_m . This is easily generalized to the situation where there are J different types of scatterers, each having its own distribution in density $N^{(j)}(z)$ and scattering coefficients $A_m^{(j)}(z)$. Then the basic results involve integrals of the form

$$\int_0^Z N(z)F\{A_m(z)\}dz = \sum_{j=1}^J \int_0^Z N^{(j)}(z)F\{A_m^{(j)}(z)\}dz$$

This allows calculations to be made for rather arbitrary distributions of inclusions, with the only restrictions being that the distributions only be a function of z and that the total concentration be small.

The results presented in this paper are only valid for small values of the concentration c . This restriction can be removed for the case of the average field, and Kaelin and Johnson¹⁴ develop a self-consistent version of the results in this paper for the coherent wave. What results is an implicit expression for the attenuation and phase, which means that an optimization problem has to be solved at each frequency. An equivalent treatment has not yet

been developed for the fluctuations in the transmitted wave. It is worth mentioning that the propagation of fluctuations can also be numerically studied by a “phase screen method”.²⁴ In that approach though the internal wave propagation effects within scatterer just partially included thus being approximated substituted by a unidirectional complex refraction coefficient. Our consideration of spherical scatterers also permits analytical results to be obtained.

Acknowledgments

This work was supported by the Assistant Secretary for Fossil Energy, Office of Oil, Gas and Shale Technologies, Federal Energy Technology Center, of the U.S. Department of Energy under Contract No. DE-AC03-76SF00098. Support was also provided by the Defense Special Weapons Agency under Grant No. DSWA-01-97-1-0026. All computations were carried out at the Center for Computational Seismology, which is supported by the DOE/BES Geoscience Program at the Ernest Orlando Lawrence Berkeley National Laboratory. Authors are grateful to two anonymous reviewers for their comments which helped to improve the paper.

Appendix A

To evaluate the integral associated with the fluctuations in the transmitted field

$$I = \int_{-\infty}^{\infty} \int_{-\infty}^{\infty} |[\mathbf{A}_{mm}(\theta, \phi)]_{c_m}|^2 \frac{dx dy}{r^2} \quad (\text{A.1})$$

it is necessary to use more accurate expressions for the scattering function $[\mathbf{A}_{mm}(\theta, \phi)]_{c_m}$ than for the case of the average field (Eq. (3.1)). We no longer can take advantage of an oscillating factor which tended to concentrate the contribution in the vicinity of $\theta \approx 0$, but must now integrate over a wider aperture, which requires a more accurate specification of the angular dependence of the scattering function. Therefore we use a scattering function in the form

$$[\mathbf{A}_{mm}(\theta, \phi)]_{c_m} = 3 \frac{j_1(\beta_m)}{\beta_m} \frac{|A_m(z)|}{|\mathbf{R}_m(0, 0)|} [\mathbf{R}_{mm}(\theta, \phi)]_{c_m}, \quad c_m = \begin{cases} z, & m = p \\ x, & m = s \end{cases} \quad (\text{A.2})$$

where $\mathbf{R}_{mm}(\theta, \phi)$ is the Rayleigh solution for the sphere of an arbitrary contrast taken from Korneev and Johnson.¹⁹ Introduction of the ratio $|A_m(z)|/|\mathbf{R}_m(0, 0)|$, with function $A_m(z)$ from Eq. (3.1) allows the applicability of Eq. (A.2) to be extended to higher frequencies while still taking advantage of the main contribution of $[\mathbf{A}_{mm}(\theta, \phi)]_{c_m}$ in Eq. (A.1) for small angles.

For an incident P wave we have

$$\frac{[\mathbf{R}_{pp}(\theta, \phi)]_z}{|\mathbf{R}_p(0, 0)|} = \cos \theta (p_1 + p_2 \cos \theta + p_3 \cos^2 \theta) \quad (\text{A.3})$$

where we have introduced the notation

$$\begin{aligned}
 p_1 &= \frac{a_1}{a_0}, \quad p_2 = \frac{a_2}{a_0}, \quad p_3 = \frac{a_3}{a_0}, \\
 a_0 &= a_1 + a_2 + a_3 \\
 a_1 &= -\frac{1}{2} \frac{\frac{3}{2}(\lambda_1 - \lambda_2) + \mu_1 - \mu_2}{\frac{3}{2}\lambda_1 + \mu_1 + 2\mu_2} + \frac{2}{3} \left(\frac{\mu_1}{\mu_2} - 1 \right) \frac{\gamma^2}{D} \\
 a_2 &= \left(\frac{\rho_1}{\rho_2} - 1 \right) \\
 a_3 &= -2 \left(\frac{\mu_1}{\mu_2} - 1 \right) \frac{\gamma^2}{D}
 \end{aligned}$$

Substituting Eq. (A.3) in Eq. (A.1) results in

$$\overline{|U_p|^2} = \int_{-\infty}^{\infty} \int_{-\infty}^{\infty} |[\mathbf{A}_{pp}(\theta, \phi)]_z|^2 \frac{dx dy}{r^2} = 2\pi |A_p(z)|^2 G_p \quad (\text{A.4})$$

where

$$G_p = \sum_{k=2}^6 g_k(w_p) P_k, \quad w_p = 2 \frac{\omega R}{v_p} \quad (\text{A.5})$$

and the coefficients P_k have the simple forms

$$\begin{aligned}
 P_2 &= p_1^2, \quad P_3 = 2p_1 p_2, \quad P_4 = 2p_1 p_3 + p_2^2 \\
 P_5 &= 2p_2 p_3, \quad P_6 = p_3^2
 \end{aligned}$$

The functions $g_k(w)$ are integrals of the form

$$g_k(w_m) = 9 \int_0^{\infty} \frac{j_1^2 \left(w_m \sin \frac{\theta}{2} \right)}{\left(w_m \sin \frac{\theta}{2} \right)^2} \cos^k \theta \frac{\rho d\rho}{r^2} = \frac{36}{w_m^2} \int_0^{\frac{w_m}{\sqrt{2}}} \frac{j_1^2(t)}{t} \left(1 - \frac{2t^2}{w_m^2} \right)^{k+1} dt \quad (\text{A.6})$$

These integrals can be analytically evaluated for low values of k . For instance, when $k = 0$ we have

$$g_0 = \frac{9}{2d^2} \left(1 + \frac{1}{d^2} - \frac{\sin 2d}{d^3} + \frac{\sin^2 d}{d^4} - \frac{4}{d^2} \int_0^d \frac{\sin^2 t}{t} dt \right), \quad d = w_m/\sqrt{2} \quad (\text{A.7})$$

As k increases the expressions for $g_k(w)$ become increasingly bulky and contain special functions similar to the g_0 case. An examination of these integral expressions revealed that,

for the purposes of this paper, the exact expressions were not necessary and the following approximate expressions were sufficiently accurate

$$\tilde{g}_k(w_m) = \frac{1}{4(k+2) \left(1 + \frac{w_m^2}{36}(k+2)\right)}, \quad k = 0, 1, 2, \dots \quad (\text{A.8})$$

Comparisons of the exact (Eq. (A.6)) and approximate (Eq. (A.8)) expressions for $k = 0, \dots, 6$ have revealed a good agreement within 5% discrepancy corridor. Note that for large arguments (high frequencies) all g_k approach the same asymptotic value

$$g_k(w_m) \approx \frac{9}{w_m^2} \quad (\text{A.9})$$

In the case of an incident S wave we have

$$\frac{[\mathbf{R}_{ss}(\theta, \phi)]_x}{|\mathbf{R}_s(0, 0)|} = S_1(\sin^2 \phi + \cos^2 \phi \cos^2 \theta) + S_2(\cos^2 \phi - \sin^2 \phi - 2 \cos^2 \phi \cos^2 \theta) \cos \theta \quad (\text{A.10})$$

where

$$s_1 = \frac{b_1}{b_0}, \quad s_2 = \frac{b_2}{b_0}, \quad b_0 = b_1 - b_2$$

$$b_1 = \left(\frac{\rho_1}{\rho_2} - 1\right) b_2 = \left(\frac{\nu_1}{\nu_2} - 1\right) \frac{1}{D}$$

Corresponding to Eq. (A.4), we have for S waves

$$\overline{|U_s|^2} = \int_{-\infty}^{\infty} \int_{-\infty}^{\infty} |[\mathbf{A}_{ss}(\theta, \phi)]_x|^2 \frac{dx dy}{r^2} = 2\pi |A_s(z)|^2 G_s \quad (\text{A.11})$$

where

$$G_s = \sum_{k=0}^6 g_k(w_s) S_k, \quad w_s = 2 \frac{\omega R}{V_{s2}} \quad (\text{A.12})$$

and the g_k functions are the same as those defined in Eq. (A.6). The coefficients S_k are given by

$$S_0 = \frac{3}{8} s_1^2, \quad S_1 = -\frac{1}{2} s_1 s_2, \quad S_2 = \frac{1}{4} (s_1^2 + 2s_2^2), \quad S_3 = 0$$

$$S_4 = \frac{3}{8} s_1^2 - s_2^2, \quad S_5 = -\frac{3}{4} s_1 s_2, \quad S_6 = \frac{3}{2} s_2^2,$$

It is easy to show that at low frequencies the functions

$$G_m(w) = G_m^{(0)}$$

do not depend on frequency and satisfy the inequalities

$$|G_m^{(0)}| < 1$$

whereas at high frequencies they approach

$$G_m(\omega) = \left(\frac{3v_m}{2\omega R} \right)^2.$$

Appendix B

The body of this paper contains expressions for the mean field and the mean squared field as it propagates through a layer containing randomly distributed scatterers. It is desirable to have similar results for the phase shift and attenuation of the propagating wave. Starting with Eq. (2.3), the primary component of the total field after interaction with a single scatterer is

$$\mathbf{u} \cdot \hat{\mathbf{u}}_m = u_{mo} + \Delta u_m^{(1)} = u_{mo} \left[1 + [\mathbf{A}_{mm}(\theta, \phi)]_{cm} \frac{e^{-ik_m(r-z)}}{r} \right] \quad (\text{B.1})$$

In terms of increments in phase and attenuation this can also be represented as

$$\mathbf{u} \cdot \hat{\mathbf{u}}_m = u_{mo} e^{(i\Delta\phi_m - \Delta q_m)} \quad (\text{B.2})$$

Assuming the change in phase and attenuation are small, this is

$$\mathbf{u} \cdot \hat{\mathbf{u}}_m \approx u_{mo} [1 + i\Delta\phi_m - \Delta q_m] \quad (\text{B.3})$$

Comparing this with Eq. (B.1) yields

$$i\Delta\phi_m - \Delta q_m = [\mathbf{A}_{mm}(\theta, \phi)]_{cm} \frac{e^{-ik_m(r-z)}}{r} \quad (\text{B.4})$$

or, equivalently,

$$\Delta\phi_m = \frac{1}{r} \text{Im}\{[\mathbf{A}_{mm}(\theta, \phi)]_{cm} e^{-ik_m(r-z)}\} \quad (\text{B.5})$$

$$\Delta q_m = -\frac{1}{r} \text{Re}\{[\mathbf{A}_{mm}(\theta, \phi)]_{cm} e^{-ik_m(r-z)}\} \quad (\text{B.6})$$

Following the same procedure used in deriving Eq. (3.1), the phase and attenuation can be averaged over a thin slab to obtain

$$i\Delta\bar{\phi}_m(z + \Delta z) - \Delta\bar{q}_m(z + \Delta z) = -i\frac{2\pi}{k_m} N(z) A_m(z) \Delta z \quad (\text{B.7})$$

This result can be converted to two differential equations which can be integrated to obtain Eqs. (3.6) and (3.7).

Next, following the same procedure used in deriving Eq. (4.2), we obtain the squared deviations

$$\Delta \overline{|\phi_m(z + \Delta z)|^2} + \Delta \overline{|q_m(z + \Delta z)|^2} = 2\pi N(z) |A_m(z)|^2 G_m \Delta z \quad (\text{B.8})$$

This can be integrated with respect to z to obtain

$$\overline{|\phi_m(Z)|^2} + \overline{|q_m(Z)|^2} = 2\pi \int_0^Z N(z) |A_m(z)|^2 G_m dz \quad (\text{B.9})$$

It is also possible to start with Eqs. (B.4) and show that so long as

$$k_m(r - z) \gg 1$$

the squared fluctuations will be evenly distributed between $\overline{|\phi|^2}$ and $\overline{|q|^2}$ and thus

$$\overline{|\phi_m(Z)|^2} = \overline{|q_m(Z)|^2} = \pi \int_0^Z N(z) |A_m(z)|^2 G_m dz \quad (\text{B.10})$$

References

1. K. Aki, "Analysis of the seismic coda of local earthquakes as scattered waves," *J. Geophys. Res.* **74**, 615 (1969).
2. K. Aki, "Scattering of P -waves under the Montana LASA," *J. Geophys. Res.* **79**, 1334 (1973).
3. K. Aki, "Scattering and attenuation of shear waves in the lithosphere," *J. Geophys. Res.* **85**, 6469 (1980).
4. L. A. Chernov, *Wave Propagation in a Random Medium*, English translation by R. A. Silverman (Dover, New York, 1960), 168 pp.
5. R. F. O'Doherty and N. A. Anstey, "Reflections on amplitudes," *Geophys. Prospect.*, **19**, 430 (1971).
6. V. A. Dubrovsky and V. S. Morozhnik, "Scattering of elastic waves from a large spherical low-contrast inclusion," *Fizika Zemli* **4**, 32 (1986).
7. S. M. Flatté and R. S. Wu, "Small-scale structure in the lithosphere and asthenosphere deduced from arrival time and amplitude fluctuations," *J. Geophys. Res.* **93**, 6601 (1988).
8. J. Groenenboom and R. Snieder, "Attenuation, dispersion, and anisotropy by multiple scattering of transmitted waves through distribution of scatterers," *J. Acoust. Soc. Am.* **98**, 3482 (1995).
9. J. E. Gubernatis, E. Domany, and J. A., Krumhansl, "Formal aspects of the theory of the scattering of ultrasound by flaws in elastic materials," *J. Appl. Phys.* **48**, 2804 (1977).
10. J. A. Hudson, "The scattering of elastic waves by granular media," *Q. J. Mech. Appl. Math.* **21**, 487 (1968).
11. J. A. Hudson, "Scattering waves in the coda of P ," *J. Geophys.* **43**, 359 (1977).
12. H. C. van de Hulst, *Light Scattering by Small Particles* (John Wiley Inc., New York, 1957), 470 pp.
13. A. Ishimaru, *Wave Propagation in Random Media* (Academic Press, 1978).
14. B. Kaelin and L. R. Johnson, "Dynamic composite elastic medium theory. Part II. Three-dimensional media," *J. Appl. Phys.* **84**, 5458 (1998).
15. L. Knopoff and J. A. Hudson, "Scattering of elastic waves by small inhomogeneities," *J. Acoust. Soc. Am.* **36**, 338 (1964).
16. L. Knopoff and J. A. Hudson, "Frequency dependence of scattered elastic waves," *J. Acoust. Soc. Am.* **42**, 18 (1967).
17. V. A. Korneev and L. R. Johnson, "Scattering of elastic waves by a spherical inclusion, I. Theory and numerical results," *Geophys. J. Int.* **115**, 230 (1993a).
18. V. A. Korneev and L. R. Johnson, "Scattering of elastic waves by a spherical inclusion, II. Limitations of asymptotic solutions," *Geophys. J. Int.* **115**, 251 (1993b).

19. V. A. Korneev and L. R. Johnson, "Scattering of P and S waves by a spherically symmetric inclusion," *Pure and Appl. Geophys.* **147**, 675 (1996).
20. G. T. Kuster and M. N. Toksöz, "Velocity and attenuation of seismic waves in two-phase media: Part 1. Theoretical formulations," *Geophysics* **39**, 587 (1974).
21. A. Lagengijk and B. van Tiggelen, "Resonant multiple scattering of light," *Physics Reports* **270**(3), 143 (1996).
22. X. Li and J. A. Hudson, "Elastic scattered waves from a continuous and heterogeneous layer," *Geophys. J. Int.* **121**, 82 (1995).
23. X. Li and J. A. Hudson, "Time-domain computation of scattering from a heterogeneous layer," *Geophys. J. Int.* **128**, 197 (1997).
24. Y. B. Liu and R. S. Wu, "A comparison between phase screen, finite-difference, and eigenfunction expansion calculations for scalar waves in inhomogeneous media," *Bul. Seism. Soc. Am.* **128**, 1154 (1994).
25. H. Sato, "Amplitude attenuation of impulsive waves in random media based on travel time corrected mean wave formalism," *J. Acoust. Soc. Am.* **71**, 559 (1982a).
26. H. Sato, "Attenuation of S waves in the lithosphere due to scattering by its random velocity structure," *J. Geophys. Res.* **87**, 7779 (1982b).
27. H. Sato, "Attenuation and envelope formation of three-component seismograms of small local earthquakes in randomly inhomogeneous lithosphere," *J. Geophys. Res.* **89**, 1221 (1984).
28. H. Sato, "Unified approach to amplitude attenuation and coda extension in the randomly inhomogeneous lithosphere," *Pure Appl. Geophys.* **132**, 93 (1990).
29. P. Sheng, *Introduction to Wave Scattering, Localization and Mesoscopic Phenomena* (Academic Press, 1995).
30. R. S. Wu, "Attenuation of short period seismic waves due to scattering," *Geophys. Res. Lett.* **9**, 9 (1982).
31. R. S. Wu, "The perturbation method in elastic scattering," *Pure Appl. Geophys.* **131**, 605 (1989).
32. R. S. Wu, "Wide-angle elastic wave one-way propagation in heterogeneous media and an elastic wave complex-screen method," *J. Geophys. Res.* **99**, 751 (1994).
33. R. S. Wu and K. Aki, "Scattering characteristics of elastic waves by an elastic heterogeneity," *Geophysics* **50**, 582 (1985a).
34. R. S. Wu and K. Aki, "Elastic wave scattering by a random medium and the small-scale inhomogeneities in the lithosphere," *J. Geophys. Res.* **90**, 10261 (1985b).